D. S. MacKenzie, Zhichao Li, B. L. Ferguson

Effect of quenchant flow on the distortion of carburized automotive pinion gears*

In this paper, the effect of quenchant flow on the distortion of carburized steel automotive pinion gears was examined using finite element software, DANTE®. Utilizing a typical heat treat rack arrangement, two parts in the quenching rack were evaluated by finite element simulations. Quenching oil velocity field around the pinion, reported in a collaborative project that applied CFD modeling of quenchant flow through the racked parts, were used to determine local heat transfer coefficients during quenching. A transverse quenchant flow direction with respect to the pinion shaft axis was studied to investigate the generation of distortion and internal stress evolution due to combined effects of thermal gradient and phase transformations. Part shape change, internal stress and phase transformation histories were calculated for this carburized pinion gear made of AISI 8620.

In dieser Arbeit wurde die Auswirkung der Durchströmung auf den Verzug von aufgekohlten Fahrzeugritzelwellen in Abschreckmedien mittels der Finite-Elemente-Software DANTE® untersucht. Zur Anwendung kam eine typische Anordnung in einem Chargiergestell. Zwei Bauteile aus diesem Chargiergestell wurden durch Finite-Elemente-Simulationen ausgewertet. Die Wärmeübergangskoeffizienten wurden aus dem mit einem CFD-Modell berechneten Strömungsfeld des Abschrecköls um die Ritzel, über das in einem Partnerprojekt berichtet wurde, ermittelt. Die Bildung von Verzug und die Entwicklung der Eigenspannungen wurden bei einer Queranströmung der Ritzelwelle durch das Abschreckmittel unter Berücksichtigung des Zusammenspiels von thermischen Gradienten und Phasenumwandlungen untersucht. Die Historie der Formänderungen, Eigenspannungen und Phasenumwandlungen wurden für diese aufgekohlte Ritzelwelle aus dem Stahl AISI 8620 (1.6523 bzw. 20NiCrMo2-2) berechnet.

1 Introduction

Heat treatment simulations of steel parts using the finite element method are being used more widely in industry due to an expended material database and improved prediction accuracy [1-4]. During a transient and highly non-linear process such as heat treatment, both thermal stress and stress generated by phase transformations work together to affect the quenching response of the component. To simulate the heat treatment process of steel parts, a thermal model, transformation kinetics models, a mechanical model, and transformation induced plasticity (TRIP) models are required, and they must share data with each other. Thermal stress, stress generated by phase transformations due to TRIP, and material volume change due to phase changes generate plastic deformations during the heating and cooling process steps, and this introduces distortion and residual stresses in the final heat treated part.

Surface heat transfer coefficients are widely used as thermal boundary conditions to drive the simulations. During a liquid quenching process, the heat transfer coefficient on the surface of the part is a combination of convection, conduction, and radiation. The vapour blanket at the early stage of quenching, and the following boiling stage complicates the thermal boundary. However, the heat transfer coefficient can be successfully approximated as a function of part surface temperature for a specific quenchant type, quenchant temperature, and agitation level. Different types of thermal probes and thermo-couple measurements on real components are also used to calculate the heat transfer coefficients using optimisation analysis and reverse calculation method [5-8].

In industry, most parts are batch heat treated in racks. Parts at different locations of the rack have different responses to quenching because of the non-uniformity of the quenchant flow pattern and local fluid temperature. The thermal boundary around a part can also be different because of the non-uniformity of quenchant flow around the specific part. Each reason mentioned above will cause scatter in heat treatment results, including distortion, residual stress, phase, and hardness distributions.

Computational fluid dynamics (CFD) modeling is starting to play a greater role in understanding the quenchant flow pattern in a quench tank, which provides important information to control the scatter in part response to heat treatment. Using the thermal boundary conditions predicted by CFD models, heat treatment simulations have been developed to predict the component response during heat treatment [9]. Crown wheels and pinion gears are widely used in automotive industries to carry high load in the transmission gear box. Because of the length of the pinion shaft, controlling bowing distortion generated by quenching is important. In this paper, pinion gears located in different locations in a quench rack are simulated using finite element software, DANTE®. CFD model results using FLUENT® were developed by collaborative project workers, and the local velocities were converted to surface heat transfer coefficients to drive the heat treatment models. The pinion gear is made of AISI 8620 steel, and it is carburized prior to quench hardening.

2 CFD modeling

Prior to heat treatment modeling, static CFD analyses were done by Fluent Inc. as part of this collaborative project, and these results are presented at this conference [10]. Three layers of pinions were included in the quenching rack as shown in Figure 1. Both the top layer and bottom layer have 16 pinions, and the middle layer contains 8 pinions. The gear teeth were not included in the CFD models. The oil flow direction is indicated in Figure 1 flowing upwards.

The oil flow rate magnitudes around the pinions in the top and middle layers are shown schematically in Figure 2. Figure 2a refers the pinions located on the top layers, and Figure 2b refers the middle layer. The oil flow rate around pinion B11 appears to be more uniform than the oil flow rate around A11, see Figure 2.

* Lecture held at the 5th Int. Conf. on Quenching and Control of Distortion and the European Conf. on Heat Treatment, 25-27 April 2007, in Berlin.

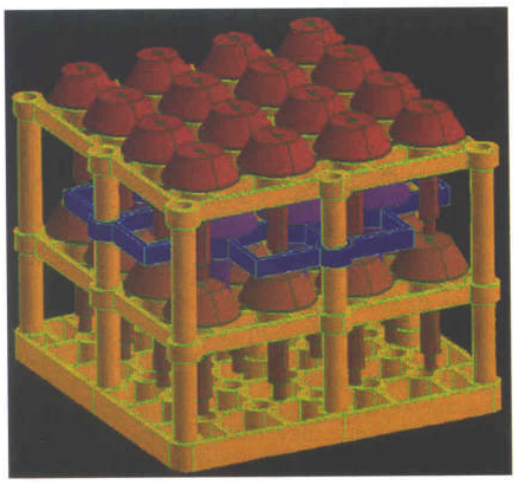

Fig. 1. Quenching rack modeling

Bild 1. Modell eines Chargiergestells

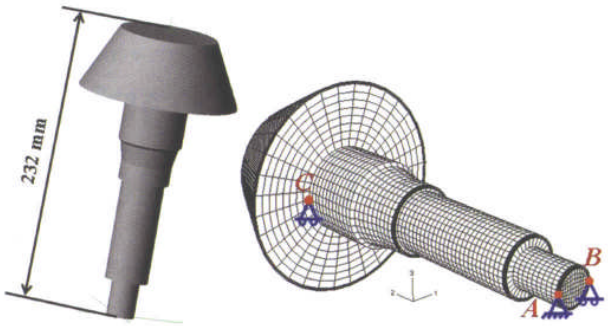

Fig. 3. Solid model and finite element meshing of pinion, a) pinion CAD model, b) finite element meshing

Bild 3. a) Massivmodell und b) Finite-Element-Netz der Ritzelwelle

These two pinions, referred as pinion A11, and B11 in later sections of this paper, were selected for heat treatment simulations using DANTE. The oil flow rates around the pinions were mapped to the heat treatment model for the thermal boundary condition calculations. More detailed description about how to convert oil flow rates around the pinion from static CFD results to a heat treatment model is shown in later section of this paper.

3 Heat treatment process modeling

The geometry of the pinion gear is shown in Figure 3a. The height of this pinion gear is about 232 mm. The gear teeth were not modeled in this study to keep the gear geometry the same for both the CFD and heat treatment models. Without modeling the gear teeth, the pinion geometry is axisymmetric. However, the oil flow around the part is not uniform during quenching. Therefore, a 3D model of the entire gear was required. The finite element mesh is shown in Figure 3b. The mesh consists of entirely of 8-noded hexahedral or brick elements. Fine surface elements were used at all the exposed surfaces to more accurately capture the surface thermal, stress and carbon gradients during heat treatment. The meshing included 51,400 brick elements and 53,939 nodes. The mechanical boundary conditions applied to the model are shown in Figure 3b. All 3 degrees of freedom were fixed at point A. At point B, degrees of freedom 2 and 3 were constrained, which allowed free expansion and contraction between point A and point B. At point C, the degree of freedom 3 was constrained to avoid rigid rotation around line AB.

3.1 Carburization process modeling

As mentioned, this pinion gear is made of AISI 8620 steel. The DANTE material database contains property data for AISI 8620 steel with carbon levels ranging from the baseline 0.2 % to values in excess 0.8 %; these data include carburization diffusivities, specific heat, thermal conductivity, phase transformation kinetics, and mechanical properties as necessary functions of carbon level, temperature and rate. More detailed information about this steel grade and material models are available in previous publications [4]. The heat treatment process for this pinion gear includes furnace heating, carburization, air transfer from furnace to quench tank, oil quenching, and finally air cooling to room temperature. The part is carburized for 8 hours in an atmosphere carbon potential of 0.8 %, and temperature of 927 °C.

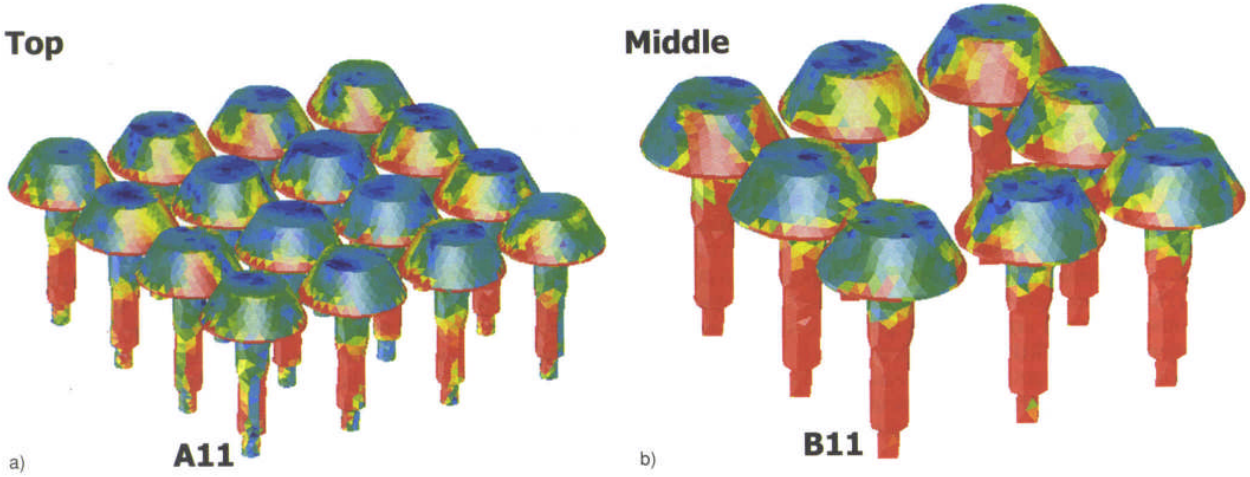

Fig. 2. Quenching oil rate magnitudes around the parts, a) top layer, b) middle layer

Bild 2. Strömungsgeschwindigkeiten des Abschreckölsum die Bauteile, a) obere Lage, b) mittlere Lage

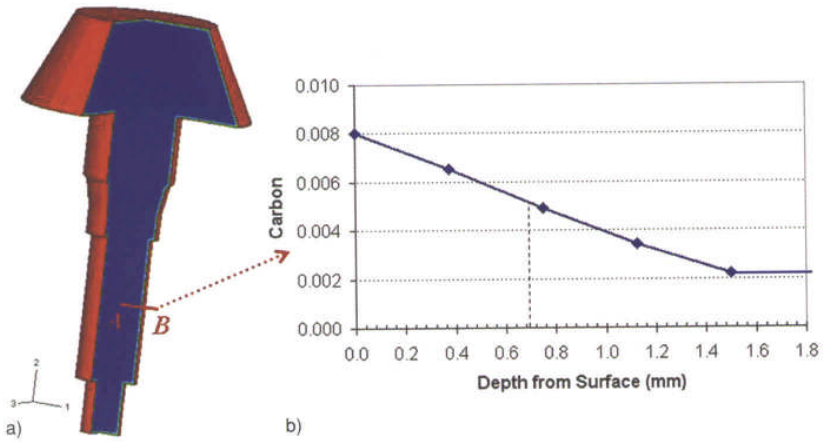

Fig. 4. Carbon distribution, a) carbon distribution contour, b) carbon distribution curve in terms of depth

Bild 4. a) Simulierte Kohlenstoffverteilung im Massivmodell, b) Kohlenstoffgehalt als Funktion des Abstands von der Oberfläche

The entire pinion surface is carburized. In Figure 4a, a quarter of the pinion mesh is removed to show the internal carbon distribution contour. Four thin brick elements are used to catch carbon gradient from the surface to the core. The carbon distribution curve after the carburization process is shown in Figure 4b. The case depth with 0.5 % carbon is about 0.7 mm.

3.2 Thermal boundary conditions

After carburization, the temperature of the pinion gears is reduced and held in the furnace at 850 °C to obtain a uniform temperature before quenching. The time required to transfer the part from furnace to the quench tank is about 10 seconds. The quench oil temperature is 120 °C. After quenching, the rack is removed and cooled to room temperature in air.

Pinions at two locations of the quench rack were simulated using DANTE, pinions A11 and B11 respectively, as shown in Figure 2. The oil flow rates around the pinions from static CFD analysis were exported in a spreadsheet that contained (x, y, z) positions of the centroids of the CFD cells surrounding the pinions and the magnitude of oil velocity. The data from the spreadsheet file was imported and mapped into DANTE model to calculate the local heat transfer coefficients for the pinion surface element faces. The relation between oil flow rate and the heat transfer coefficient is described using equation (1).

$$h_c = h_{oil} \cdot v^n \tag{1}$$

where h_c is the oil flow rate dependent heat transfer coefficient, h_{oil} is the average oil heat transfer coefficient, v is the oil flow rate, and the exponential n equals 0.466 in this study. The heat transfer coefficient h_{oil} in equation (1) is a function of part surface temperature, which also represents the vapour blanket, nucleate boiling, and convection phenomena during oil quenching.

A third heat treatment model simulated a quench process with transverse oil flow direction as shown in Figure 5. The oil flow rate around the part was higher on the side facing the oil flow and lower on the opposite side. The heat transfer coefficient varied as a sine wave in the circumferential direction and was not dependent on axial position.

4 Results and discussion

Distortion generated during heat treatment reduces the quality of the part, generally by reducing fatigue life and increasing service noise. Severe distortion leads to excessive scrap rates. Understanding the underlying causes of distortion during heat treatment is important. Finite element modeling of the heat treat process steps provides a clear and efficient way to understand the part response during heat treatment, which is also helpful for eliminating severe distortion problems. Quenching is a transient and highly non-linear process. During quenching, high internal stresses are generated from the thermal gradients and metallurgical phase transformations. Plastic deformation caused by high internal stress leads to permanent distortion in the part after quenching.

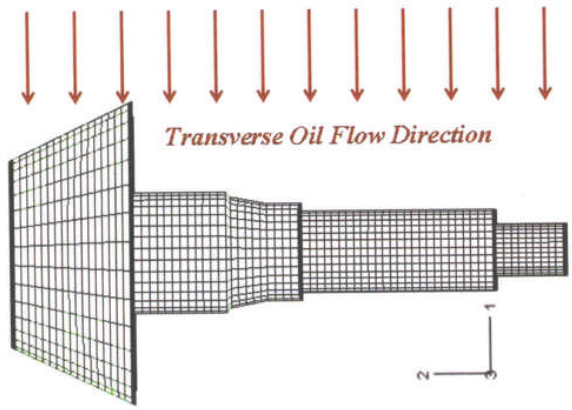

Fig. 5. Transverse oil flow direction for the third DANTE simulation

Bild 5. Queranströmung durch das Abschreckӧl für die dritte Dante-Simulation

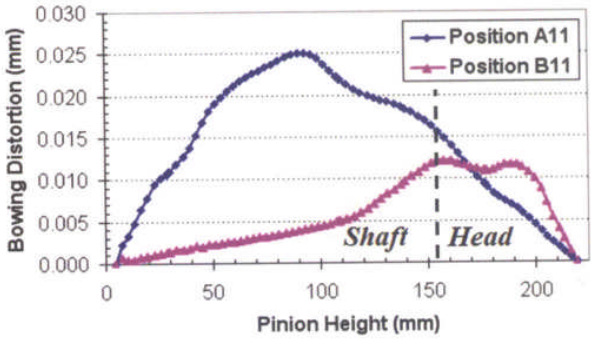

Fig. 6. Comparison of distortions for pinion A11 and pinion B11

Bild 6. Vergleich der Verzüge von Ritzelwelle A11 und B11

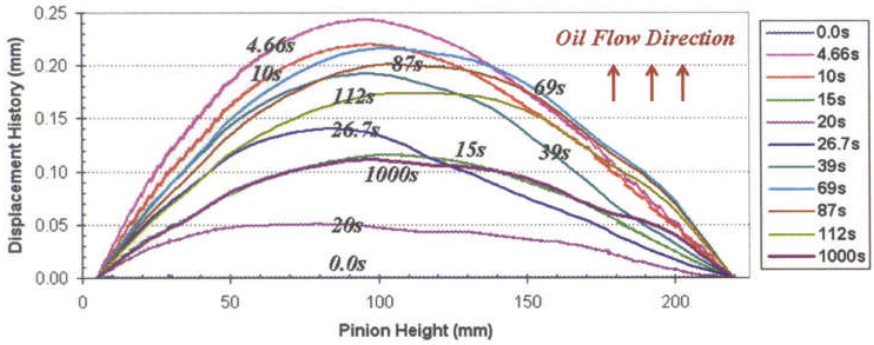

Fig. 7. Bowing displacements at different times during quench with transverse oil flow direction

Bild 7. Durchbiegung im Verlauf der Abschreckung mit Queranströmung

4.1 Distortion comparison between pinion A11 and pinion B11

In this study, distortion is defined as the magnitude of bowing displacement of the pinion gear axis. Figure 6 compares the final distortion of pinion A11 and pinion B11 in the as-quenched condition. The x-axis in Figure 6 is the height of the pinion with the head of the pinion on the right side, and the y-axis is the bowing distortion. The bowing distortion of pinion A11 is about 0.025 mm, and the bowing distortion of pinion B11 is about 0.012 mm. In general, the predicted oil velocity around part B11 from the CFD model is more uniform than the oil flow around part A11. A more uniform rate of oil flow around the part tends to reduce the quenching distortion by producing more uniform cooling. However, the oil flow rate around the head of pinion A11 is more uniform than the rate around the heat of pinion B11. From DANTE heat treatment simulation results shown in Figure 6, the bowing distortion in the head of pinion B11 is more than that of pinion A11, which agrees the CFD oil velocity pattern.

The results of the CFD and FEA model were validated using sixty actual heat treated loads (2400 parts) racked in an identical as the modeled heat treated load. The distortion of the parts were measured and compared to the predicted results. The results are shown in Table 1.

The results show excellent correlation between the predicted distortion of the shaft and the actual measured distortion of the shaft. Previously, using a different racking method, the distortion was high, and for these parts was typically 0.1–0.2 mm. The use of modeling and subsequent validation using production furnaces achieved an immediate and substantial cost savings, and reduced the distortion one-hundred fold. Savings were estimated in the millions of Euro.

One area for improvement in terms of heat transfer coefficient application relates to mesh size. Because the CFD model has to simulate the entire tank and basket of parts, the mesh size was much larger than the fine size needed by the heat treatment model. The use of a CFD sub-model that applies a finer mesh around the part to be modeled would improve the determination of surface heat transfer coefficients and the subsequent accuracy of distortion and residual stress state predictions.

Position	Predicted (mm)	Actual (mm)		
		Maximum	Average	Minimum
A11	0.025	0.020	0.011	0.008
B11	0.015	0.017	0.009	0.005

Table 1. Results comparing the predicted shaft distortion with the actual distortion of the heat treated pinions, when racked identically to the model. Previous racking method produced distortion as high as 0.2 mm.

Tabelle 1. Vergleich des vorhergesagten Verzugs mit den tatsächlich aufgetretenen Verzügen an wärmebehandelten Ritzelwellen bei identischer Chargierung. Durch die ursprüngliche Chargierung wurden Verzüge bis zu 0,2 mm erzeugt.

4.2 Transverse oil flow case study

During a quenching process with an overall oil flow in the transverse direction, as shown in Figure 5, the difference of oil flow rate around the circumference of the shaft and head is more than the velocity differences of pinions A11 and B11. The predicted bowing distortion in this case is more than 0.10 mm. Because of the predicted large distortion generated by the transverse oil flow pattern, this part orientation relative to the quenchant flow direction is rarely used in industry for this pinion gear or shafts in general. However, because of the predicted large bowing distortion and the simplicity of this oil flow pattern as compared to the flow patterns for pinions A11 and B11, the transverse oil flow case was used to investigate how distortion is generated by the non-uniformity of temperature field, phase transformations, and internal stress evolutions during quenching.

The internal stresses generated by the thermal gradient and phase transformations are the main cause of plastic deformation and subsequent distortion. Figure 7 shows the bowing displacements of the pinion at different holding times in quench. Figure 8 shows the austenite and temperature distributions at different quenching times. Figures 7 and 8 are used together to explain how the thermal gradient and phase transformations contribute to the bowing distortion. The heating process can cause large distortion for parts with large variance of section size [1]. However, for this pinion gear, the axial bowing distortion caused by furnace heating and carburization process is ignorable according to DANTE simulations. In Figure 7, the x-axis is the height of the pinion, and y-axis is the bowing displacements. Different curves in Figure 7 represent the axial bowing displacements at different holding times in quench. The curve for 0.0 s is pinion bowing distortion after furnace heating, carburization, and 10 seconds air transfer from furnace to quench tank; this is the start of immersion quenching and no bow is noted.

The consequence of transverse oil flow is shown in both Figure 7 and Figure 8a. At the beginning of the quenching process, the pinion surface facing the oil flow (referred to as *front side I* in later sections) is cooled faster than the opposite side (referred to as *back side* in later sections), and the front side contracts more than the back side. As a result of the thermal contraction, severe bowing occurs at this early quenching time, as shown by the curve for 4.66 s in Figure 7. The surface carbon of the pinion is about 0.8 %, as shown in Figure 4b. The martensitic transformation start temperature (Ms) of AISI 8680 is about 205 °C. At the quench time of 4.66 seconds, the minimum temperature of the part is about 330 °C, which is higher than the Ms temperature of the part surface. As a result, there is no phase transformation occurring before 4.66 seconds in quench; as shown in Figure 8a the part remains 100 % austenite. The thermal stress in the surface of the pinion at early quenching time causes plastic deformation.

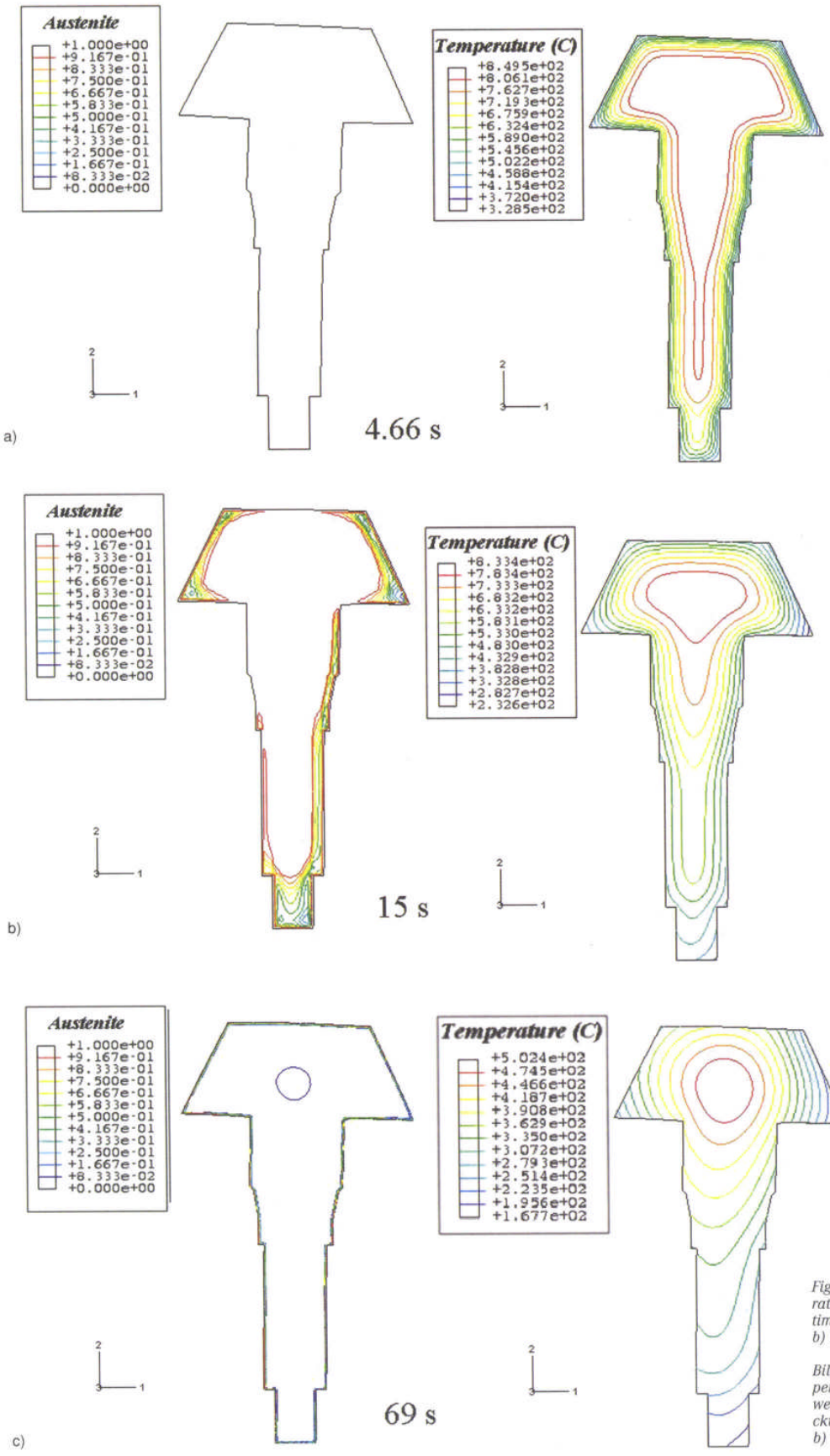

Fig. 8. Austenite and temperature distributions at different times in quench, a) 4.66 seconds b) 15 seconds c) 69 seconds

Bild 8. Austenitanteil und Temperaturverteilung in der Ritzelwelle im Verlauf der Abschreckung, a) 4,66 Sekunden, b) 15 Sekunden, c) 69 Sekunden

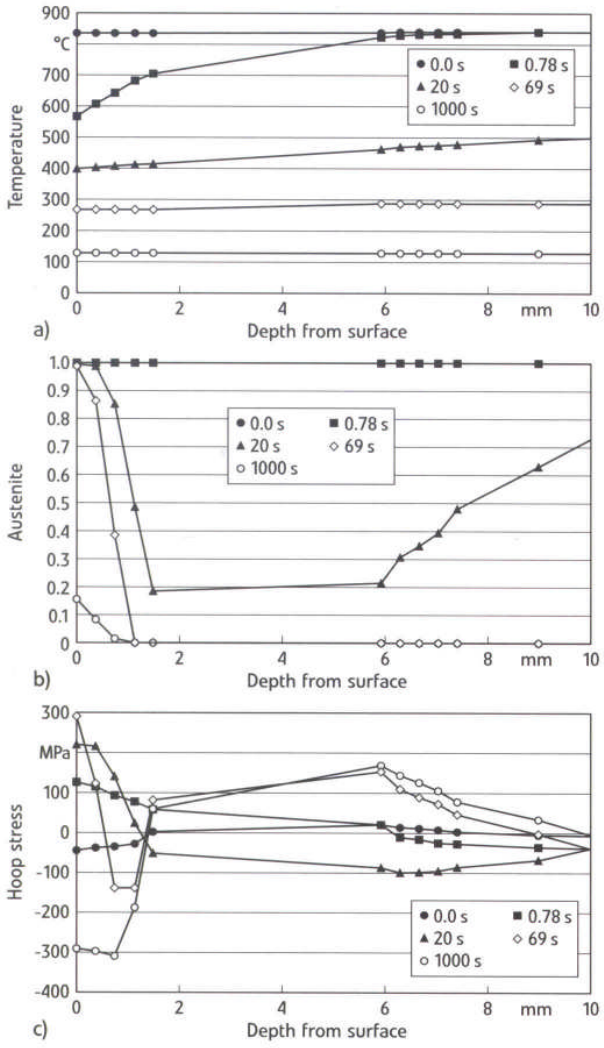

Fig. 9. Stress evolution during quenching

Bild 9. Entwicklung der Eigenspannungen im Verlauf der Abschreckung

While the temperature on the front side continues to drop, the rate of cooling slows and the cooling rate on the back side catches up and exceeds the cooling rate on the front side. The material on the back side contacts more than the front side during this time period, which leads to a reduced bowing. A limited amount of phase transformation occurs beneath the carburized case layer, with the phase transformation starting earlier on the front side. Also, the material volume expansion caused by the phase transformation tends to reduce the axial bowing distortion. The reduction of axial bowing distortion with increased time is a combination of thermal stress and phase transformation effects, with the thermal effect contributing more to the pinion shape change during the first 10 seconds in quench. Between 10 s and 20 s in the quench, a greater amount of phase transformation occurs on the front side than the back side of the pinion, which is shown by the austenite distribution contour in Figure 8b. The cooling rate difference between the front and back sides during this time period is reduced with increasing time. The material volume expansion due to phase transformations tends to reduce the bowing distortion, as shown by the curves for 10 s, 15 s, and 20 s in Figure 7. During this time period, the phase transformation has a more significant effect on the pinion shape change than the temperature difference between the front side and back side.

With continued cooling, the phase transformation rate on the back side increases and eventually exceeds the phase transformation rate on the front side. More material volume expansion occurs on the back side, which increases the bowing displacement, as shown by the curves for 20 s, 26.7 s, 39 s, and 69 s in Figure 7. During this time period, the phase transformation timing difference between the front side and back side dominates the shaft bowing displacements.

After 69 seconds in quench, most phase transformations are done except for the high carbon surface in the case, as shown by the austenite distribution contour in Figure 8c. However, the temperature of the back side is still higher than the temperature of the front side. By continued holding of the pinion in the quench tank, the back side cools more than the front side. Greater thermal contraction occurs on the back side than the front side of the pinion during this time period, which decreases the bowing distortion as shown by the curves for 87 s, 112 s, and 1000 s in Figure 7. During this time period, a small amount of phase transformation occurs, and the thermal gradient is the main cause of the pinion shape change.

Residual stress distribution after quenching is an important quenching property. In general, high surface compressive residual stress is desired to improve the fatigue life of the part. In this paper, nodes located on line AB in Figure 4 are selected to investigate the effect of temperature gradient and phase transformation on internal stress evolution during quenching. In Figure 9, the x-axis is the depth of the nodes (located on line AB Figure 4) from the OD surface of the pinion gear. The y-axes are temperature, volume fraction of austenite and hoop stress, respectively. During 10 second air transfer from furnace to quench tank, the temperature on the surface of the pinion drops slightly, as shown by the 0.0 second curve in Figure 9a. The pinion is 100 % austenite at the end of air transfer, and the internal stresses are minor as shown in Figure 9c.

After 0.78 seconds in the quench oil, the surface temperature has dropped to 560 °C. There are no phase transformations occurring at this time. The thermal contraction of the pinion surface introduces a 120 MPa tensile stress on the surface, as shown by the curve with solid square marks in Figure 9c. To balance the surface tensile stress, the core of the pinion is in a slightly compressive state. As mentioned, the pinion has been carburized, and the predicted carbon distribution is shown in Figure 4b. AISI 8620 with base carbon has a Ms temperature of 415 °C, and the same steel grade with 0.8 % carbon (AISI 8680) has a Ms temperature of 205 °C. The isothermal Time-Temperature-Transformation (TTT) diagrams for AISI 8620 and AISI 8680 show that the diffusive transformations of higher carbon content require much longer incubation time, and the rate of diffusive transformation is much lower than that of baseline or core carbon content [4]. After 20 seconds in the quench oil, the surface temperature has dropped to about 400 °C. No phase transformations are occurring at or near the surface. However, bainite formation has started under the carbon case, as shown by the 20 seconds curve in Figure 9b. The volume expansion due to bainite formation under the carbon case generates a compressive stress of about 100 MPa at this location, as shown in Figure 9c. To balance the compressive stress at this location, a tensile stress of about 220 MPa has developed at the surface. With further cooling in the quench tank, the temperature on the surface drops to 260 °C at 69 seconds, and the temperature gradient between the surface and the core is small. After holding for 69 seconds in quench, martensite formation has occurred in the deeper case layers which have lower carbon

contents, where the temperature is lower than the Ms of the corresponding carbon level. As shown in Figure 9b, the martensitic transformation in deeper case introduces high compressive stress around this region. The material volume expansion due to martensite formation in this region causes tensile stress in the austenite on the surface of the pinion, where no phase transformation has yet occurred. Because austenite has low yield strength elative to subsurface martensite and bainite, the surface austenite is deformed plastically to relieve the surface stress; this generates a surface tensile strain. At 69 seconds into the quench, phase transformations have been completed at all locations except the high carbon surface layer. When the surface temperature drops below Ms with further cooling, the surface austenite transforms to martensite. The material volume expansion due to martensite formation generates a compressive stress of 300 MPa in the surface, as shown by the curve for 1000 seconds in Figure 9c.

5 Summary

The heat treatment process of a pinion gear was studied using finite element software DANTE®. As part of this study, a static CFD model was conducted by Fluent Inc. to predict the oil flow pattern around parts positioned in a rack for batch hardening. The local oil flow rates reported by CFD results were converted to local heat transfer coefficients to drive the heat treatment models. Two data sets from CFD results that represented rack locations for two pinion gears were used to develop simulations for these specific locations. Results have shown that the corner position of the middle layer the rack (B11) has less distortion than the corner position of the top layer (A11). The overall level of bowing distortion was predicted to be less that 0.025 mm. Further CFD sub-modeling with a finer mesh around the part to be modeled during heat treatment is required to improve the correlation between CFD modeling results and heat treatment models.

A third study with transverse oil flow pattern was simulated using DANTE to more easily understand how distortion and residual stresses were generated during quenching. Relations among carbon gradient, thermal gradient, and phase transformation sequence were studied. The underlying bases for distortion was the non-uniformity of cooling of the part and the effect that this had on the level of thermal stress and on the timing of phase transformations in the part.

The authors would like to thank Fluent Inc. for their CFD modeling works, and provides the modeling results to DANTE modeling. The authors also would like to thank Andrew Freborg for his help on converting the quenchant flow rate from static CFD modeling results to heat transfer coefficients.

References

1. *Li, Z.; Ferguson, B. L.; Freborg, A. M.:* Data Needs for Modeling Heat Treatment of Steel Parts. Proc. of Materials Science and Technology Conf., MS&T 2004, New Orleans, La./USA, *Baker, M. A.* (ed.); Association for Iron and Steel Technology, Warrendale, Pa./USA, p. 219-226
2. *Freborg, A. M.; Li, Z.; Ferguson, B. L.; D. Schwam, D.:* Improving the Bending Fatigue Strength of Carburized Gears. Proc. of Materials Science and Technology Conf., MS&T 2004, New Orleans, La./USA, *Baker, M. A.* (ed.); Association for Iron and Steel Technology, Warrendale, Pa./USA, p. 227-234
3. *Ferguson, B. L.; Freborg, A.; Petrus, G.:* Software Simulates Quenching. Adv. Mater. Process. *158* (2000) 2, H31-H36
4. *Shun Zhang; Li, Z.; Ferguson, B. L.:* Effect of Carburization on the Residual Stress and Fatigue Life of a Transmission Shaft. Proc. 23rd ASM Heat Treating Society Conf., Sept. 25-28, 2005, Pittsburgh, PA/USA, *Herring, D.* (ed.), p. 216-223
5. *Bates, C. E.; Totten, G. E.:* Application of Quench Factor Analysis to Predict Hardness Under Laboratory and Production Conditions. Proc. 1st Int. Conf. on Quenching and Control of Distortion, Sept. 22-25, 1992, Chicago, Illinois/USA, *Totten, G. E.* (ed.); ASM Int., Materials Park, p. 33-39
6. *Varde, A. S.; Rundensteiner, E. A.; Maniruzzaman, M.; Sisson, R. D.:* Estimating Heat Transfer Coefficients as a Function of Temperature by Data Mining. Proc. 23rd ASM Heat Treating Society Conf., Sept. 25-28, 2005, Pittsburgh, PA/USA, *Herring, D.* (ed.), p. 348-357
7. *Narazaki, M.; Asada, S.; Fukahara, K.:* Recent Research on Cooling Power of Liquid Quenchants in Japan. Proc. 2nd Int. Conf. on Quenching and the Control of Distortion, Nov. 4-7, 1996, Cleveland, Ohio/USA, *Totten, G. E.* (ed.); ASM Int., Materials Park, p. 37-46
8. *Shick, D.; Chenoweth, D.:* Development of Carburization and Quenching Simulation Tool: Determination of Heat Transfer Boundary Conditions in Salt. Proc. 2nd Int. Conf. on Quenching and the Control of Distortion, Nov. 4-7, 1996, Cleveland, Ohio/USA, *Totten, G. E.* (ed.); ASM Int., Materials Park, p. 357-366
9. *MacKenzie, D. S.; Kumar, A.; Metwally, H.:* Optimizing Agitation and Quench Uniformity using CFD. Proc. 23rd ASM Heat Treating Society Conf., Sept. 25-28, 2005, Pittsburgh, PA/USA, *Herring, D.* (ed.), p. 271-278
10. *Kumar, A.; Metwally, H.; MacKenzie, D. S.:* Evaluation of Flow Uniformity around Automotive Pinion Gears During Quenching. Proc. 5th Int. Conf. on Quenching and Control of Distortion, and Europ. Conf. on Heat Treatment, April 25-27, 2007, Berlin, *Grosch, J.* et al. (eds.), p. 69-76

The authors of the paper

D. Scott Mackenzie: Houghton International Inc., Madison and Van Buren Avenues, Valley Forge, PA 19482 USA

Zhichao Li: Deformation Control Technology, Inc., 7261 Engle Road, Suite 105, Cleveland, OH 44130 USA

B. Lynn Ferguson: Deformation Control Technology, Inc., 7261 Engle Road, Suite 105, Cleveland, OH 44130 USA

Manuscript submitted: October 2007.

Dieser Beitrag hat die Dokumentennummer HT100445 und steht unter www.HTM-Journal.de für Sie zum Download bereit.